

Effect of carrier-induced hydrogenation on the passivation of the poly-Si/SiO_x/c-Si interface

Cite as: AIP Conference Proceedings **1999**, 040026 (2018); <https://doi.org/10.1063/1.5049289>

Published Online: 10 August 2018

Yang Yang, Pietro P. Altermatt, Yanfeng Cui, Yunyun Hu, Daming Chen, Lijuan Chen, Guanchao Xu, Xueling Zhang, Yifeng Chen, Philip Hamer, R. Sebastian Bonilla, Zhiqiang Feng, and Pierre J. Verlinden



[View Online](#)



[Export Citation](#)

ARTICLES YOU MAY BE INTERESTED IN

[Realization of TOPCon using industrial scale PECVD equipment](#)

AIP Conference Proceedings **1999**, 040018 (2018); <https://doi.org/10.1063/1.5049281>

[Controlling P and B diffusion during polysilicon formation](#)

AIP Conference Proceedings **1999**, 040011 (2018); <https://doi.org/10.1063/1.5049274>

[Increasing the photo-generated current in solar cells with passivating contacts by reducing the poly-Si deposition temperature](#)

AIP Conference Proceedings **1999**, 040015 (2018); <https://doi.org/10.1063/1.5049278>

AIP | Conference Proceedings

Get **30% off** all
print proceedings!

Enter Promotion Code **PDF30** at checkout



Effect of Carrier-Induced Hydrogenation on the Passivation of the poly-Si/SiO_x/c-Si Interface

Yang Yang¹, Pietro P. Altermatt^{1, a)}, Yanfeng Cui⁴, Yunyun Hu¹, Daming Chen¹, Lijuan Chen¹, Guanchao Xu¹, Xueling Zhang¹, Yifeng Chen¹, Philip Hamer², R. Sebastian Bonilla², Zhiqiang Feng¹, and Pierre J. Verlinden³

¹*Changzhou Trina Solar Energy Co., Ltd., State Key Laboratory for Photovoltaic Science and Technology (SKL), No.2 Trina Road, Trina PV Park, Xinbei District, Changzhou 213031, China*

²*University of Oxford, Department of Materials, 16 Parks Road, Oxford OX1 3PH, United Kingdom*

³*Now with Amrock Pty Ltd, PO Box 714, McLaren Vale, SA 5171, Australia*

⁴*Now with GCL, No.88 Yangshan Road Economic Development Zone, Xuzhou, Jiangsu, China*

^{a)}Corresponding author: pietro.altermatt@trinasolar.com

Abstract. In the progress made in understanding carrier-induced degradation and regeneration in p-type mono and multi silicon solar cells, it was implied that hydrogen passivates certain defects during illuminated anneals at temperatures between 150-350°C. However, there are only few reports on the effect of carrier-induced regeneration (CIR) in n-type material. In this work, we apply a CIR treatment on samples structured as poly-silicon/tunnel oxide/n-type CZ. We present evidence suggesting that hydrogen passivation plays an important role in the regeneration process, and that improvement does not occur in the Si bulk but mainly at the Si/SiO_x interface. For n-type poly, the Si/SiO_x interface improves at temperatures of 250°C and above regardless of illumination and H-containing dielectric layer, and the rate of improvement is merely accelerated by illumination. For p-poly, the Si/SiO_x interface is only stable in our experiments if the H-containing dielectric layer is present during CIR.

INTRODUCTION

Lifetime instabilities in n-type wafers have been mainly attributed to thermal donors. It is well known that processing temperatures between 450°C and 550°C generate a variety of thermal donors, which can be mostly dissolved with an anneal at 600°C for 15 – 20 minutes [1]. These thermal donors may be generated during ramping down after high-temperature processing. Because they increase the fill factor of the IV curve [2], they are often tolerated. Apart from thermal donors, n-type materials attracted much less attention in terms of hydrogen passivation, although hydrogen increases the diffusivity of interstitial oxygen and may lead to more thermal donors.

Recently, high-efficiency cells have become limited by recombination at the contacts, and thus passivated contacts have received great attention for moving along the roadmap to higher efficient cells. Hydrogen passivation has been found critical for passivated contacts cells [3, 4, 5, 6]. In these studies, H was found to be able to reach the interface of the tunnel oxide/Si or i-layer/c-Si and to passivate it well.

This work aims to gain better understanding of the role of carrier-induced hydrogenation of the interface between the tunnel oxide and the n-type Cz wafer. In the following, we are going to show the experimental details of carrier-induced recombination (CIR) of three groups of samples, followed by the discussion of results and a simulation of hydrogen transport for n-poly Si samples.

EXPERIMENTS

Sample Preparation

Three groups of wafers were prepared as following.

- Group A: Symmetrical samples were prepared on 170 μm thick 6 inch n-type CZ wafers with 5 Ωcm resistivity. These wafers were put in a TMAH solution for saw damage removal and polishing, followed by a standard RCA cleaning procedure. Then the wafers were loaded into a LPCVD furnace to thermally grow a ~ 1.5 nm thin oxide and an in-situ phosphorus doped a-Si layer on top with a thickness of 200 nm. A subsequent annealing step was performed at 900°C in nitrogen atmosphere to turn the a-Si layer into a poly-Si layer. Afterwards, a 80 nm thin SiN_x layer was deposited by PECVD on the top of n-poly Si. However, during the SiN_x layer deposition, half of the 156×156 mm² wafer was masked by a 78×156 mm² dummy wafer so there is no dielectric layer on that half. Subsequently, these samples obtained fast firing in a conveyer belt furnace at a peak temperature of 740°C. The wafers were laser-cut into quarters so two pieces obtained the firing with SiN_x and two pieces without SiN_x .
- Group B: Symmetrical samples were prepared on 170 μm thick 6 inch n-type CZ wafers with 10 Ωcm resistivity. These wafers were put in a TMAH solution for saw damage removal and polishing, followed by a standard RCA cleaning procedure. Then the wafers were loaded into a LPCVD furnace to thermally grow a ~ 1.5 nm thin oxide, and a 340 nm intrinsic a-Si layer on top. The tunnel oxide and the a-Si layer were both grown at 570°C for 10 min and 105 min, respectively. In one group of these wafers, a PSG layer was then deposited on both sides of samples in a POCl_3 furnace and annealed (driven-in) at 880°C in nitrogen atmosphere in order to dope the n-poly Si layer. In another group of these wafers, the poly-Si layer was doped by a 20 min BBr_3 diffusion at 850°C and annealed (driven-in) at 880°C in nitrogen atmosphere for 2 hours. Afterwards, both groups of samples obtained a 15 nm thin AlO_x and a 52 nm thin SiN_x layer by PECVD deposition on the top of poly-Si, followed by a slow firing step in a conveyer belt furnace at a peak temperature of 650°C. After firing, some of these wafers were dipped in HF to remove the $\text{AlO}_x/\text{SiN}_x$ layers.
- Group C: Same as group B, but the p-poly Si layer was removed by single-side wet chemical etching. Hence, these are one-sided p-poly samples.

CIR Treatment and Monitoring of Samples

A homemade regeneration box with a temperature-controlled hot plate and a white LED light source is used for the CIR experiment. The temperature of the hot plate is fixed at various levels between 150°C and 350°C, and the light intensity stays constant near 1 sun irradiance. The wafers were taken out of this box in intervals and τ_{eff} was measured with a Sinton WCT-120 lifetime tester. The dopant diffusion profiles were measured with the ECV method using wafer profiler CVP21 tool.

RESULTS, DATA EVALUATION, AND DISCUSSION

Figure 1 shows the results of Group A. Two quarter pieces (one with SiN_x , the other without) obtained a CIR by illumination at $\sim 200^\circ\text{C}$, the two other quarter pieces (again, one with SiN_x , the other without) were not illuminated while at $\sim 200^\circ\text{C}$. Only the piece that had both a SiN_x layer during firing and illumination during annealing shows an increase in quality, i.e. an increase of τ_{eff} . In contrast, absence of illumination does inhibit quality improvement, even if the SiN_x was present during firing.

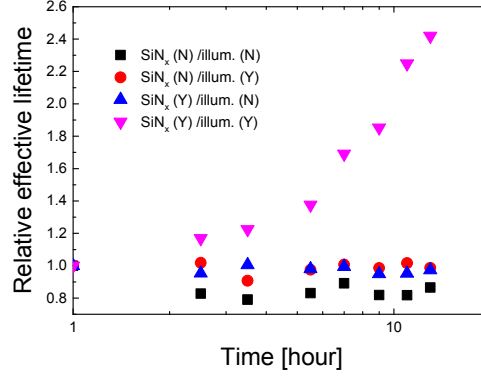


FIGURE 1. Relative changes of the effective lifetime of samples from Group A, under the condition of 200°C, with or without SiN_x and with or without illumination.

To find out whether τ_{eff} increases mainly due to surface passivation or whether also a significant amount of bulk passivation is involved, we used another sample from Group A and extended the regeneration time to 43 hours until τ_{eff} became saturated. We fit the measured τ_{eff} curves with SRH and device theory:

$$\frac{1}{\tau_{\text{eff}}} = \frac{1}{\tau_{\text{SRH}}} + \frac{1}{\tau_{\text{Au}}} + \frac{1}{\tau_{\text{rad}}} + \frac{2J_0(N_{\text{dop}} + \Delta n)}{qWn_i^2} \quad (1)$$

The saturation current density of the surface, J_0 [7], is measured from the inverse slope of τ_{eff} [8]. To make sure that the measured J_0 values are not influenced by Auger recombination, we extract them at the injection of $3 \times 10^{15} \text{ cm}^{-3}$. Usually, τ_{SRH} is neglected because it is unknown (and assumed to be not injection-dependent [9]). However, we fit τ_p , contained in the well-known SRH formula for τ_{SRH} , self-consistently in Eq. (1). The value for τ_n does not influence τ_{eff} as long as there is $\tau_n < 40 \text{ ms}$ (assuming the defect state is near mid gap). In the fitting procedure, all τ_{eff} measurements in Fig. 2(a) can be fitted very precisely using $\tau_p = 36 \text{ ms}$ (lines) except the initial τ_{eff} measurement (green). This means that, during the first hour of CIR treatment, the bulk lifetime improves from the initial green line, fitted self-consistently with J_0 , from $\tau_p = 6 \text{ ms}$ ($\tau_n < 3 \text{ ms}$) to $\tau_p = 36 \text{ ms}$ and then stays constant. This indicates strongly that, after one hour of CIR, the increased τ_{eff} was solely due to improved surface passivation, as shown in Fig. 2(b).

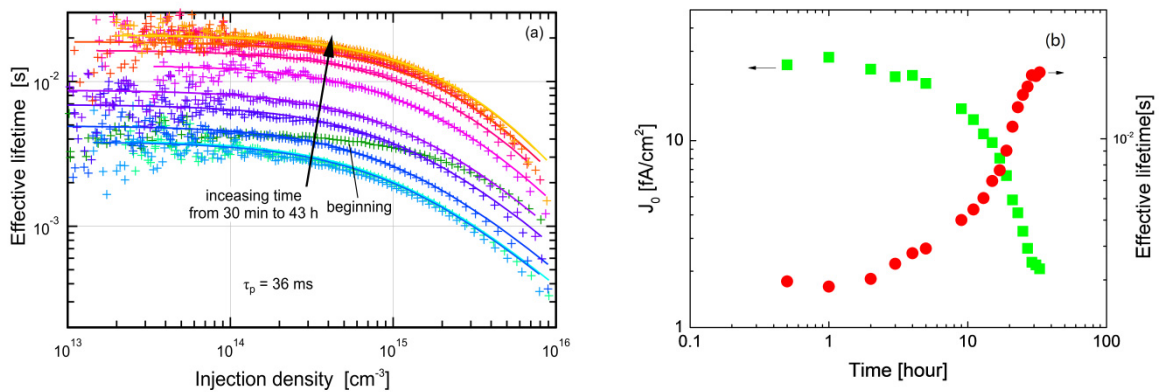


FIGURE 2. (a): measured τ_{eff} (symbols) and calculated τ_{eff} with Eq. (1) using the same bulk SRH parameter τ_p (lines) for all times after 0.5, 1, 5, 11, 15, 21, 25, 31, 35, 41 and 43 hours of treatment. (b): effective lifetime τ_{eff} at an injection density Δn of $3 \times 10^{14} \text{ cm}^{-3}$ and J_0 at $\Delta n = 3 \times 10^{15} \text{ cm}^{-3}$ as a function of CID time.

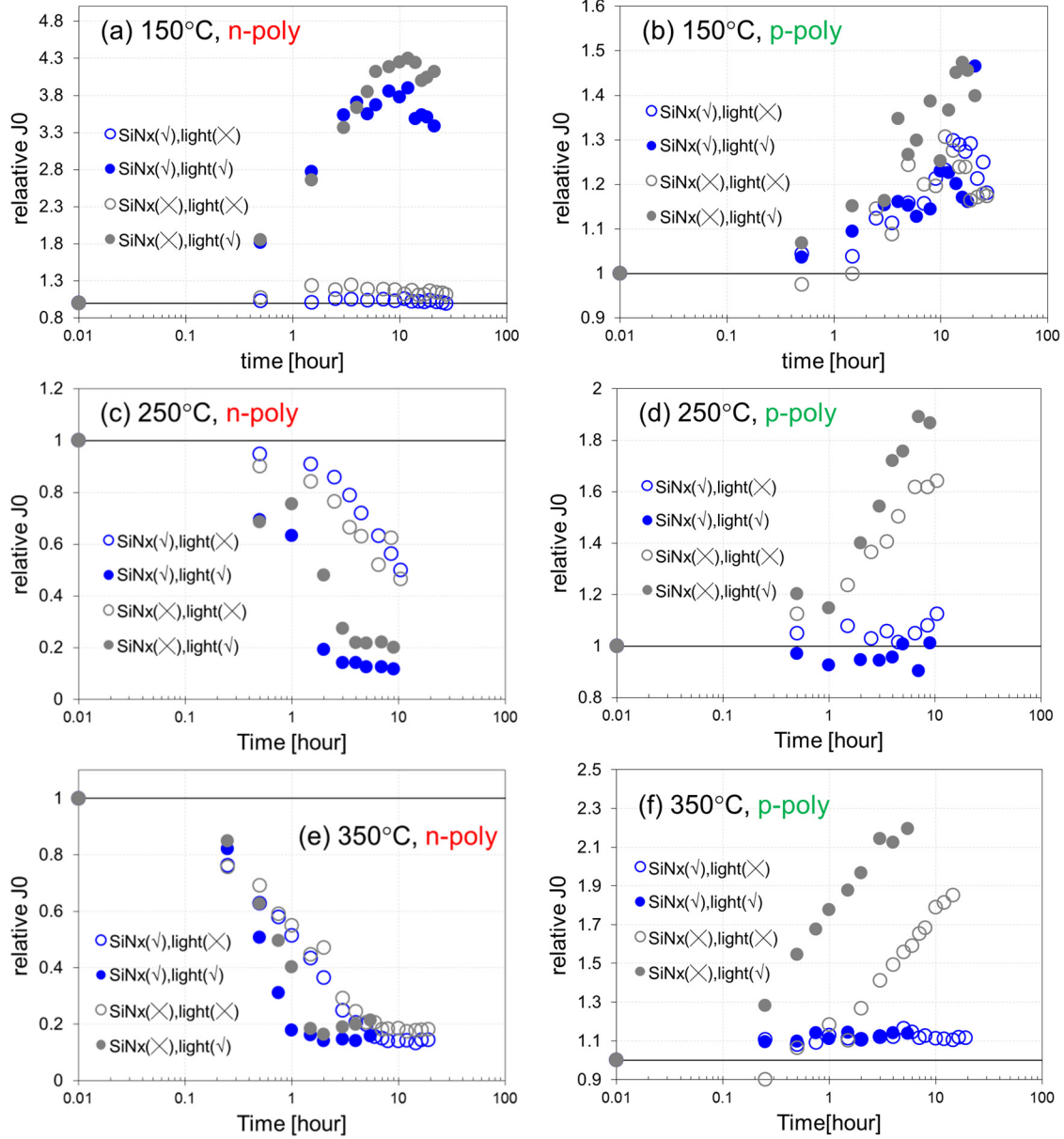


FIGURE 3. Changes of relative J_0 for n-poly/tunnel oxide and p-poly/tunnel oxide samples after CIR treatment at temperatures of 150°C, 250°C and 350°C respectively

With the group B samples, we investigated the influence of temperature on n-type and p-type poly-Si samples. Fig. 3 (a), (c) and (e) show the measured relative J_0 change at the indicated temperatures for the symmetrical n-poly Si/tunnel oxide/c-Si samples. Samples with/without SiNx are indicated in blue/grey (referring to their appearance), samples in light/dark conditions are indicated as filled/empty symbols. The following behaviour of the samples containing an n-poly layer is found:

1. At the lowest temperature ($\sim 150^\circ\text{C}$), CIR degrades the interface quality, regardless whether there is a nitride layer or not. In the dark, there is no change. But, after 10 hours, surface quality start to improve, indicating a very slow regeneration process.
2. At both higher temperatures ($\sim 250^\circ\text{C}$ and $\sim 350^\circ\text{C}$), surface quality improves regardless whether there is a nitride layer or illumination or neither of these.
3. The differences between with or without nitride are rather small, but under illumination, a nitride accelerates the improvement slightly.

4. The differences between light and dark start to vanish at the highest temperature.
5. Generally, all improvements occur faster under illumination at higher temperature.

The relative J_0 change measured for samples containing p-poly layers instead of n-poly layers are shown in Fig. 3 (b), (d) and (f):

6. At the lowest temperature ($\sim 150^\circ\text{C}$), surface quality degrades regardless whether there is a nitride or illumination or neither of them.
7. At both higher temperatures ($\sim 250^\circ\text{C}$ and $\sim 350^\circ\text{C}$), the nitride layer stabilizes the interface quality, regardless whether there is illumination or not.
8. The samples without nitride still degrade, and faster at higher temperature.

Comparing n-poly and p-poly samples:

9. the nitride layers accelerate quality improvements only slightly with n-poly, while the nitride layers make a large difference in p-poly samples;
10. illumination accelerates changes in n-poly samples at lower temperatures, but not so much at high temperatures, while in p-poly layers, illumination degrades quality but only in samples without nitride layer.

These differences make hydrogen a candidate for explaining the behavior, because in n- or p-type, different hydrogen charge states predominate. In addition it is expected that the total amount of hydrogen present in a given region of a device structure will depend on the doping profile. First, we investigate the role of the nitride as a hydrogen source by modeling hydrogen diffusion from the nitride layer into the Si wafer during firing. The rate of hydrogen release from the nitride into the Si wafer, R_H , was measured in [10,11], and the H bond density in the nitride layers was measured in [12-15]. We conclude from these publications that the hydrogen release is faster with higher refractive index n because a higher amount of hydrogen is bound to Si instead of nitrogen; the Si-H binding energy is smaller (3.3 eV) than the N-H binding energy (4 eV) according to [16, 17]. The data for R_H given by [10] and [11] and shown in Fig. 4(a) cannot be fitted with an Arrhenius function using the binding energies as activation energies because the hydrogen is not set free but incorporated into the Si lattice. We therefore guess the activation energy E_{act} to be 0.9 eV so it qualitatively describes the experiments of the samples that received PECVD nitrides in [10-15]: the hydrogen release rate was found negligible below 300°C , and a significant amount of H was released only above 400°C . We adjust the prefactor of the Arrhenius function, $R_{H,0}$, so it describes the differences observed with the different refractive indices in the experiments (for example $R_{H,0} = 1 \times 10^{10} \text{ cm}^{-2}\text{ns}^{-1}$ for $n = 1.9$, up to $1 \times 10^{12} \text{ cm}^{-2}\text{ns}^{-1}$ for $n = 2.4$). The slow-firing of our low-temperature paste occurs at about 650°C (for 10 seconds), hence we choose $R_H = 10^3 \text{ cm}^{-2}\text{ns}^{-1}$ for our nitrides having $n = 2.05$ as a lower estimate ($10^5 \text{ cm}^{-2}\text{ns}^{-1}$ would be an upper estimate).

We model the diffusion of the released hydrogen with the model described in [18]. The concentration profiles of the various charge states of atomic H at the end of firing are shown in Fig. 4(b), together with the concentration profiles of the H dimer as well as of hydrogen bound to the phosphorus dopants. We compare these modeling results with the steady state concentrations given by the analytical theory of [19], where we used the modeled H^0 profile as input because it is largely independent of depth. The concentrations of all charge states coincide rather precisely with [19], meaning that steady state is approached after 10 s of firing at 650°C in the samples covered with an n-poly layer. Only the H^+ concentration is significantly lower than in steady-state, possibly due to the small supply of H^+ through the n-poly layer. Note the abundance of H^- at the SiO_x interface, and that H^0 and H^+ also exist in considerable amounts. We were unable to simulate the diffusion of H through the p-poly layer with the model of [18], which was probably due to the difficulties for H to penetrate the p-poly layer. The steady-state concentrations of the H charge states are very different in the layers covered with the p-poly layer [19]: there exists mainly H^+ and very little H^- , but illumination (carrier injection) increases H^- . The primary reason is the asymmetry of the hydrogen donor and acceptor levels within the bandgap. The donor level (+/0) is shallow below the conduction band edge, the acceptor level (0/-) is at midgap [20]. Considering the Fermi energies, it is much easier to have H^+ in n-type than H^- in p-type. Indeed in lightly doped n-type, H^+ dominates at elevated temperatures.

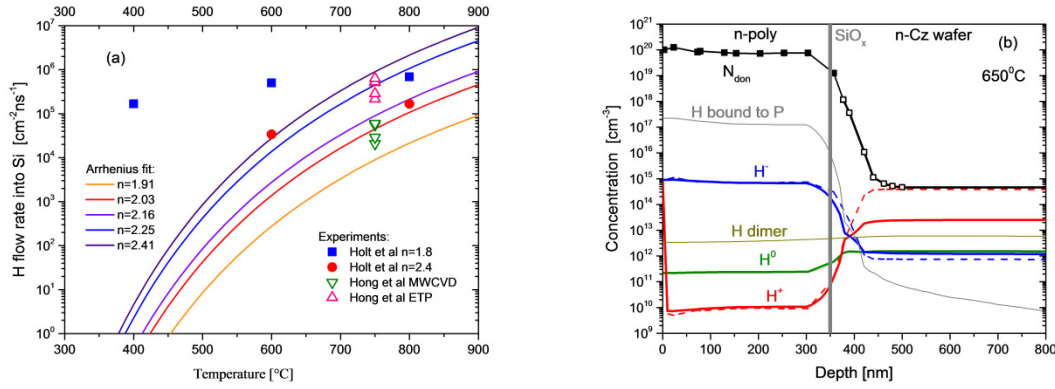


FIGURE 4. (a): The rate of hydrogen release from the SiN_x layer into the Si bulk as reported [10,11] from experiments (symbols), and a sophisticated guess for PECVD-deposited nitride samples (lines). (b): The concentration of various hydrogen species after firing for 10 s at 650°C, simulated in transient with the model in [18] (solid lines), and a comparison with the steady-state analytical theory of [19] (dashed lines).

For interpretation of our J_0 measurements, we now consider which charge states of H are able to passivate which types of defects at the Si/SiO_x interface. The capture cross-sections for electron and hole capture, σ_n and σ_p , are mainly given by the charge states of the dangling bonds and only to a lesser extent by the shapes of the molecular orbitals. From [21] and [22] we conclude that the main two defect types that dominate the overall recombination at the Si/SiO_x interface are the P_L and the P_H dangling bonds having one oxygen or two oxygen back bonds, respectively, making these defects donor-like, i.e. positively charged and hence having $\sigma_n > \sigma_p$. Because these defect types are donor-like and not amphoteric, it might be difficult to passivate them with H⁺, instead of H⁻. With this and the above modeling we finally conclude that our n-poly samples have an abundance of H⁻ and hence a low and decreasing J_0 , while our p-poly samples are deprived of H⁻ and only illumination (carrier injection) delivers a sufficient amount of H⁻ to passivate the dangling bonds if a nitride layer is present. Further work needs to be conducted to investigate the concentration and the role of H⁰ in the passivation of SiO_x at p-poly layers. To explain the behavior of J_0 with temperature transport mechanisms of H may play an important role: at temperatures below firing, hydrogen tends to want to move from the bulk back to the interface due to a change in drift/diffusion ratio and trapping in the highly doped region. This flow of H may contribute that the passivation improves with low temperature annealing. Illumination may accelerate this by reducing the amount of H trapped at phosphorus dopants through carrier injection. Another possibility is that hydrogen passivation of the interface has a reasonably low binding energy and so tends to not satisfy all bonds during firing, whereas at low temperature, providing there is enough H⁻, passivation may improve as it is much less likely to break these bonds once formed.

After our explanations, we now test to which extent the nitrogen layer may release hydrogen through the p-poly layer, because it may be that the H⁻ concentration is a steady-state concentration influenced by illumination (carrier injection) and not by the H release from the nitride layer. We therefore covered only one or none of the two wafer surfaces with a p-poly layer while keeping the deposition of the nitrogen layer on both sides as before. Figure 5 shows the measured τ_{eff} (evaluating J_0 of the surface is more involved in asymmetric samples). Indeed, the sample with one side of p-poly has the highest τ_{eff} , because H released from the other side with no p-poly layer can readily diffuse through the wafer during firing and deliver H⁻ to the SiO_x underneath the p-poly layer.

With our main interpretation that the dangling bonds of the Si/SiO_x interface are deprived from H⁻ for passivation, we can also explain an experiment from 2005 [23]. There, it was found that SiO₂ passivation of boron-diffused surfaces is instable: after storing the samples in the dark for two years, the passivation quality was gone and could only be recovered with a forming gas anneal (FGA). Because Al₂O₃ passivation was introduced soon after that experiment, the issue of instable SiO₂ passivation on boron-diffused surfaces was not further investigated. Now we conclude that the deprivation of H⁻ is the main cause for the observed instabilities.

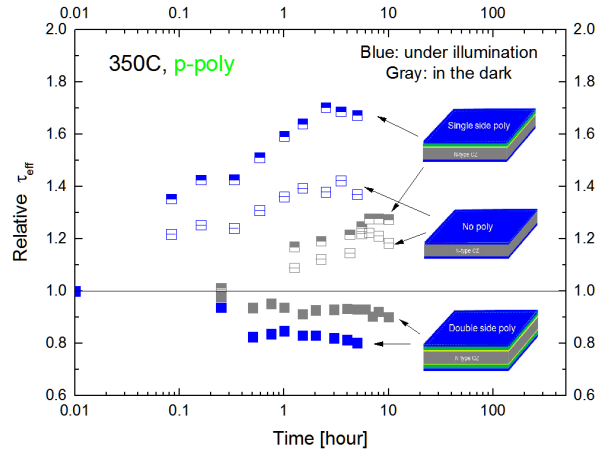


FIGURE 5. Measured effective lifetime during CID of samples in Group C that only obtained a p-poly layer on one side or none at all.

CONCLUSION

Carrier-induced regeneration (CIR) treatment has been tried on samples structured as poly-silicon/tunnel oxide/n-type CZ. A detail and self-consistent SRH lifetime fitting show that the degradation/improvement does not occur in the Si bulk but mainly at the Si/SiO_x interface. For n-type poly, the Si/SiO_x interface passivation degrades at temperature of 150°C under illumination, but improves at temperatures of 250°C and above regardless of illumination and H-containing dielectric layer and the rate of improvement is merely accelerated by illumination. For p-poly, the Si/SiO_x interface is only stable in our experiments if the H-containing dielectric layer is present during CIR. These behaviours might be explained by the re-distribution of H after high temperature firing process, especially the H⁻, considering the dominating defects at Si/SiO_x interface are donor like so that they can hardly passivated by H⁺. This work also shed a light on a possible way to improve passivating contact solar cells.

ACKNOWLEDGMENTS

This work is supported by the Natural Science Foundation of Jiangsu Province under the Project Number of BK20150276.

REFERENCES

1. C. S. Fuller and R. A. Logan, *J. Appl. Phys.* 28, 1427 (1957).
2. W. Duan, S. Yuan, Y. Sheng, W. Cai, Y. Chen, Y. Yang, P.P. Altermatt, Z. Feng, P.J. Verlinden, "A route towards high efficiency n-type PERT solar cells", Proc. 32nd European Photovoltaic Solar Energy Conference, Munich, Germany, 2016, pp. 399–402.
3. S. Lindekugel, H. Lautenschlager, T. Ruof, S. Reber, in: Proceedings of the 23rd European Photovoltaic Solar Energy Conference, Valencia, Spain, 2008, pp. 2232.
4. Descoeudres, Antoine, et al. "Improved amorphous/crystalline silicon interface passivation by hydrogen plasma treatment." *Applied Physics Letters* 99.12 (2011).
5. F. Feldmann, et al. "The application of poly-Si/SiO_x contacts as passivated top/rear contacts in Si solar cells." *Solar Energy Materials and Solar Cells*. 159, 265–271 (2017).
6. Larionova, Yevgeniya, et al. "On the recombination behavior of p+ type polysilicon on oxide junctions deposited by different methods on textured and planar surfaces." *physica status solidi (a)* 214.8 (2017).
7. K. R. McIntosh and L. E. Black, *J. Appl. Phys.* 116, 014503 (2014).

8. D. E. Kane and R. M. Swanson, "Measurement of the emitter saturation current by a contactless photoconductivity decay method," Proc. 18th IEEE Photovoltaic Specialists Conference (IEEE, NY, 1985), pp. 578–583.
9. B. Liu, Y. Chen, Y. Yang, D. Chen, Z. Feng, P. P. Altermatt, P. Verlinden, H. Shen, [Solar Energy Materials and Solar Cells](#) 149, 258–265 (2016).
10. J. K. Holt, D. G. Goodwin, A. M. Gabor, F. Jiang, M. Stavola and Harry A. Atwater, [Thin Solid Films](#) 430, 37–40 (2003).
11. J. Hong, W. M. M. Kessels, W. J. Soppe, A. W. Weeber, W. M. Arnoldbik, M. C. M. van de Sanden, [J. Vac. Sci. Technol. B](#) 21, 2123–2132 (2003).
12. F. Jiang, M. Stavola, A. Rohatgi, D. Kim, J. Holt, H. Atwater and J. Kalejs, [Appl. Phys. Letters](#) 83, 931–933 (2003).
13. S. Kleekajai, F. Jiang, M. Stavola, V. Yelundur, K. Nakayashiki, A. Rohatgi, G. Hahn S. Seren and J. Kalejs, [J. Appl. Phys.](#) 100, 093517 (2006).
14. J. F. Lelièvre, E. Fourmond, A. Kaminski, O. Palais, D. Ballutaud, M. Lemiti, [Solar Energy Materials and Solar Cells](#) 93, 1281–1289 (2009).
15. H. Mäckel and R. Lüdemann, [J. Appl. Phys.](#) 92, 2602–2609 (2002).
16. Z. Yin and F. W. Smith, [Phys. Rev. B](#) 43, 4507–4510 (1991).
17. F. de Brito Mota, J. F. Justo, and A. Fazzio, [J. Appl. Phys.](#) 86, 1843–1847 (1999).
18. P. Hamer, B. Hallam, R. S. Bonilla, P. P. Altermatt P. Wilshaw and S. Wenham, [J. Appl. Phys.](#) 123, 043108 (2018).
19. C. Sun, F. E. Rougieux, and D. Macdonald, [J. Appl. Phys.](#) 117, 045702 (2015).
20. C. Herring, N. Johnson, and C. G. Van de Walle, [Phys. Rev. B](#) 64, 125209 (2001).
21. W. Füssel, M. Schmidt, H. Angermann, G. Mende, H. Flietner, [Nuclear Instruments and Methods in Physics Research A](#) 377, 177–183 (1996).
22. J. Albohn, W. Füssel, N. D. Sinh, K. Kliefoth, and W. Fuhs, [J. Appl. Phys.](#) 88, 842–849 (2000).
23. P. P. Altermatt, H. Plagwitz, R. Bock, J. Schmidt, R. Brendel, M. J. Kerr, A. Cuevas, "The surface recombination velocity at boron-doped emitters: comparison between various passivation techniques, " Proc. 21st European Photovoltaic Conference (Dresden, Germany, 2006, WIP Munich), pp. 647–650.